

# In-Situ Study of Creep Induced Stress in Magnesium Alloys

Michelle Fletcher<sup>1</sup>, Lukas Bichler<sup>1</sup>, Dmitry Sediako<sup>2</sup>

<sup>1</sup> Mechanical Engineering, UBC Okanagan, Kelowna, British Columbia, Canada V1V 1V7

<sup>2</sup> NRC Canadian Neutron Beam Centre, Chalk River Laboratories, Chalk River, ON, Canada K0J 1J0

Ever increasing demand for energy efficient, yet high performance vehicles in the automotive and aerospace industries has resulted in a high demand for light weight structural components. Magnesium (Mg) alloys are the lightest structural materials available with a high specific strength. Further, Mg alloys are easy to machine and cast, with a good potential for recycling [1], establishing themselves as good candidate materials for diverse industrial applications. However, Mg alloys do not have the required creep resistance for automotive applications with operating temperatures above 125°C [2]. This restriction greatly limits their use for automotive components, such as engine block parts, where the greatest impact on fuel efficiency and performance could be achieved [3]. The poor creep strength has been traditionally related to grain boundary movement and plastic deformation which leads to inter-granular failure [4].

The addition of aluminum (Al) has been known to increase castability and room temperature strength; however, this strength drastically diminishes above 120°C [1]. The addition of rare earth elements (REs) such as lanthanum, praseodymium, cerium, and neodymium are known to increase creep resistance of Al-containing Mg alloys. The addition of strontium (Sr) to Al-containing Mg alloys has a similar effect on the creep resistance as adding REs while at a lower material cost. During this research two Al containing alloys were analyzed including the industrial benchmark for creep resistant alloys AE42 and a Sr containing alloy AJ32.

In the Al-free alloys, Zinc (Zn) addition to Mg alloys increases room temperature strength and raises the eutectic temperature. The increased eutectic temperature raises the alloy operating temperature [5]. However, Zn addition also increases the alloy's susceptibility to microporosity and embrittlement [6], thus negatively affecting alloy performance. The addition of REs to Zn-containing Mg alloys increases creep resistance and decreases the susceptibility to

microporosity and alloy embrittlement [7]. The Al-free alloy analyzed during this research was ZE10.

**Table 1** Nominal Compositions of AE42, AJ32 and ZE10

	AE42 (wt%)	AJ32 (wt%)	ZE10 (wt%)
Al	3.5-4.5	3-3.5	≤0.05
Zn	≤0.2	≤0.2	0.8-1.2
Mn	0.2-0.5	0.2-0.5	0.2-0.5
Fe	≤0.01	≤0.01	≤0.01
Ni	≤0.005	≤0.005	≤0.005
Cu	≤0.05	≤0.05	≤0.05
Si	≤0.05	≤0.05	≤0.05
RE	1.5-2.5		0.3-0.7
Ca			
Sr		1.5-2.5	
Zr			0.45-0.7
Ce	0.9		0.2
La	0.3		0.1
Nd	0.2		0.1
Pr	0.5		0.01
Mg	Balance	Balance	Balance

The AE42, AJ32 and ZE10 alloys were produced by Timminco Corp., and their nominal compositions are provided in Table 1. The three alloys studied (AE42, AJ32 and ZE10) were processed via hot extrusion. No processing defects, such as cracking or solute segregation were observed. Material samples were machined to a 15mm length with a 6mm diameter.

The experiments were performed on the L3 spectrometer. Compressive creep testing was performed on each alloy under a 50 MPa load at 175°C. This testing hoped to expose the material to the extreme environmental conditions for further material comparison.

A germanium monochromating crystal was used to direct a single 1.792 Å wavelength of neutrons towards the sample. The first neutron diffraction measurements occurred at room temperature and low applied stress.

The lowest possible applied stress was 200 N as this was the load necessary to hold the sample within the vice of the compression apparatus. The temperature was increased in 50°C intervals, while maintaining the 200 N load. The temperature was increased gradually to avoid overheating of the material sample. Upon heating, the material expanded and the lattice spacing increased due to thermal strain. Neutron diffraction measurements were taken for the  $(10\bar{1}0)$ ,  $(0002)$ ,  $(10\bar{1}1)$ ,  $(10\bar{1}2)$ , and  $(2\bar{1}\bar{1}0)$  atomic planes at each temperature interval to measure the amount of thermal strain upon heating.

Once the thermal strains were measured up to 175°C a load of 1411 N was applied to the sample, while maintaining the temperature at 175°C. These conditions were held constant for 23-33 hours while neutron diffraction testing was performed. During this time, the lattice spacing was measured at each plane repeatedly to analyze lattice spacing during material creep.

Once the 23-33 hours of creep testing was complete, the load was released and the lattice strain after unloading was measured. The temperature was then released back to room temperature and the strains upon cooling were compared to those of the sample measured prior to the application of the 1411 N load.

The neutron diffraction data, gained from each measurement, took the form of neutron flux versus diffraction angle. A curve was fitted to this data and the peak of this curve was used as the measured angle of diffraction. The diffraction angle was then used to calculate lattice spacing using Bragg's Law. The value of  $d_0$  was taken as the lattice spacing at room temperature under a 200 N load.

The extensometer data collected while a 1411 N was applied under 175°C for each of the three samples can be seen in Figure 1. As can be seen AE42 had the highest strain, followed by AJ32 and ZE10 had the highest creep resistance.

The lattice strain measurements versus the time from the beginning of material creep for AE42, AJ32 and ZE10 in the  $(10\bar{1}0)$  plane can be seen in Figure 2. The microstrain increased upon the raise in temperature, as expected under thermal strain. The lattice spacing then decreased upon the application of stress, at the beginning of material creep, and remained constant for all three alloys during the creep duration. The lattice spacing then increased once the load was released and decreased back to the initial value once the temperature dropped back to room temperature.

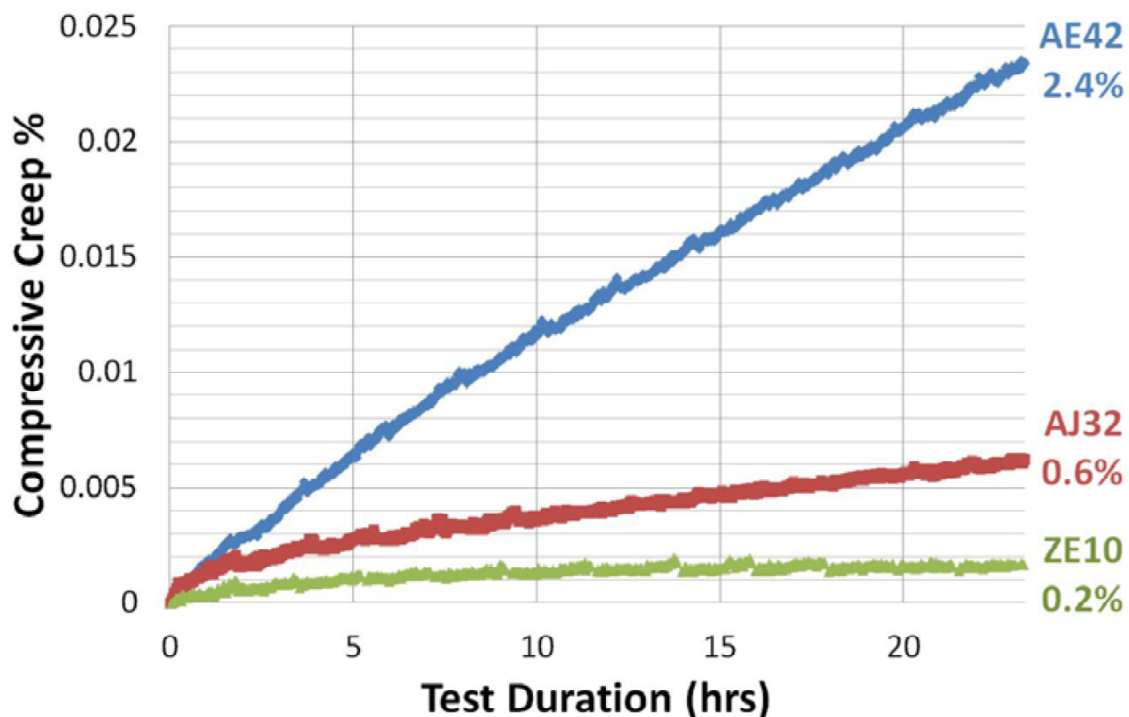


Fig. 1 Compressive creep measured with extensometer during testing

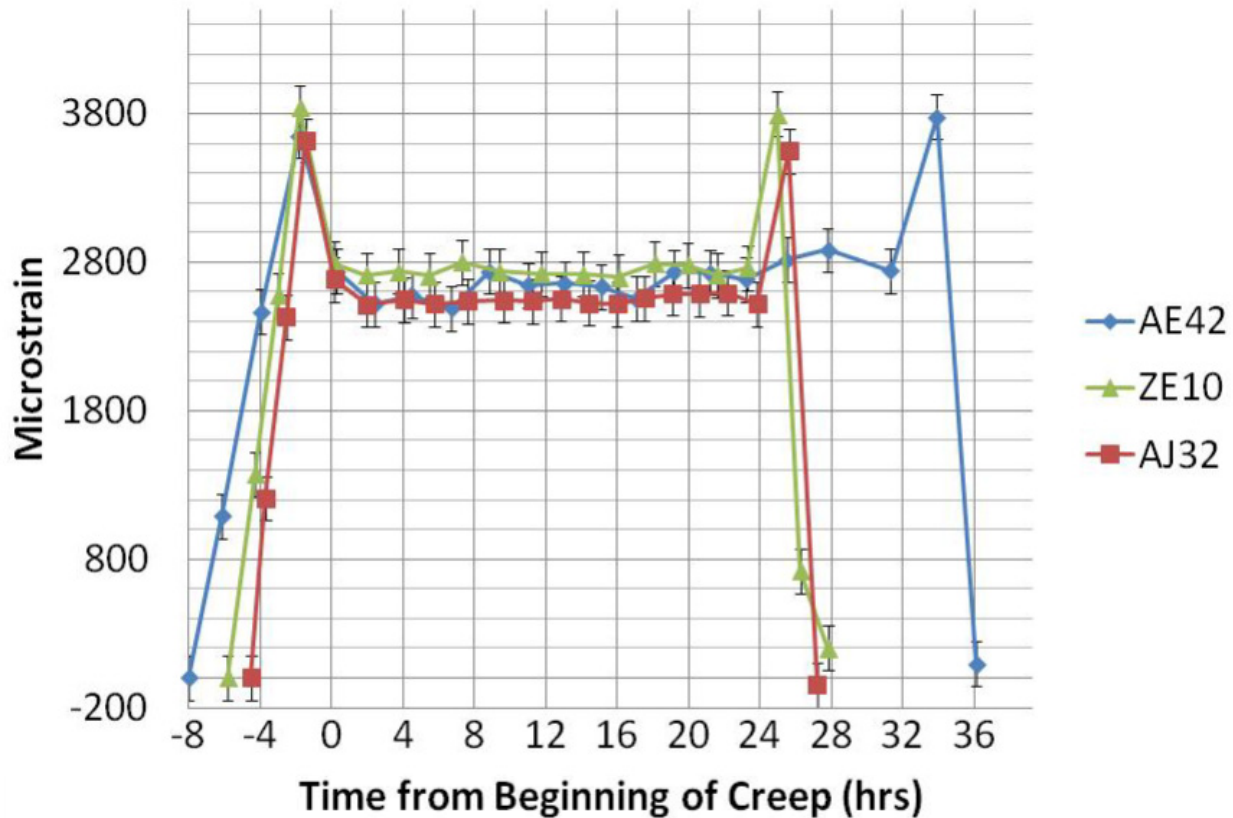


Fig. 2 (10 $\bar{1}0$ ) microstrains measured using neutron diffraction

The constant microstrain during creep, while the extensometer measured material deformation, indicates that all material creep consisted of plastic deformation. The fact that the microstrain returned to zero for all alloys once the temperature and stress loads were released also indicated a lack of residual strain present after testing. Similar figures were made for each of the five planes measured during testing.

Neutron diffraction testing was followed by a metallographic analysis to determine mechanisms for creep strength within the alloys. The intermetallic compounds present in the alloys were analyzed to have a significant role on creep resistance.

#### References

- [1] Michael Avedesian, and Hugh Baker, ASM Specialty Handbook; Magnesium and Magnesium Alloys (Materials Park, OH: ASM International, 1999).
- [2] Q. Guo et al., "Elevated temperature compression behavior of Mg-Al-Zn alloys," *Materials Science and Technology*, 22 (6) (2006), 725-729.
- [3] Edward F. Emley, *Principles of Magnesium Technology* (Long Island City, NY: Pergamon Press, 1966).
- [4] J. Yan et al., "Creep deformation mechanism of magnesium-based alloys," *Journal of Material Science*, 43 (2008), 6952-6959.
- [5] T. Rypaev et al., "Microstructure of superplastic QE22 and EZ33 magnesium alloys," *Materials Letters*, 62 (2008), 4041-4043.
- [6] H. Deming et al., "Indentation creep behavior of AE42 and Ca-containing AE41 alloys," *Materials Letters*, 61 (2007), 1015-1019.
- [7] B.R. Powell et al., "Microstructure and creep behavior in AE42 Magnesium die-casting alloy," *Journal of Metals*, 54 (8) (2002), 34-38.